



# Unraveling the Underwater Morphological Features of Roncador Bank, Archipelago of San Andres, Providencia and Santa Catalina (Colombian Caribbean)

Javier Idárraga-García\* and Hermann León

*Oceanographic and Hydrographic Research Center of Colombia, Cartagena, Colombia*

## OPEN ACCESS

### Edited by:

Santiago Herrera,  
Lehigh University, United States

### Reviewed by:

Federico Di Traglia,  
Università degli Studi di Firenze, Italy  
Aggeliki Georgiopoulou,  
University College Dublin, Ireland

Jon J. Major,  
United States Geological Survey,  
United States

### \*Correspondence:

Javier Idárraga-García  
jidarragag@unal.edu.co

### Specialty section:

This article was submitted to  
Marine Conservation  
and Sustainability,  
a section of the journal  
Frontiers in Marine Science

**Received:** 29 August 2018

**Accepted:** 11 February 2019

**Published:** 25 February 2019

### Citation:

Idárraga-García J and León H  
(2019) Unraveling the Underwater  
Morphological Features of Roncador  
Bank, Archipelago of San Andres,  
Providencia and Santa Catalina  
(Colombian Caribbean).  
*Front. Mar. Sci.* 6:77.  
doi: 10.3389/fmars.2019.00077

In this study, we present the first detailed description of the morphology of the Roncador Bank deep underwater environments, located in the central sector of the SeaFlower Biosphere Reserve (Archipelago of San Andres, Providencia and Santa Catalina-ASAPSC, Republic of Colombia). The analysis was carried out from multibeam bathymetric information recently acquired by the Oceanographic and Hydrographic Research Center of Colombia (CIOH), and the subsequent creation of a 35 m-resolution digital terrain model, which was the main input for the geomorphological mapping. The results allowed to determine that Roncador Bank corresponds to a seamount of highly irregular contour, reaching a height up to 2,350 m with respect to the surrounding seafloor. The volcanic edifice that makes up the seamount is bounded to the south and east by two escarpments, which are tectonically related with the Southern Roncador and Eastern Roncador faults, respectively. We were able to determine that these faults are currently active and that recently have generated earthquakes of magnitudes up to 6.0, which has important implications for the estimated seismic risk in the ASAPSC. This situation allowed to infer that the volcanic processes that formed the Roncador volcano were controlled by the presence of major faults on the seabed. The steep slope gradients (up to 40°) of the escarpments effectively concentrate erosive processes, leading to the development of a dense gully network and extensive slope deposits in the hillsides. Also, we identified debris-avalanche deposits indicating the occurrence of partial collapses of Roncador, which shows that gravity-driven mass transport processes have played an important role in the edifice shaping. These large-scale underwater landslide events may have the capacity to generate tsunamis, so it is necessary to carry out specific studies to analyze their tsunamigenic potential. Finally, the mapping and detailed description of Roncador seamount morphological features, such as pinnacles, escarpments, hummocky terrains, ridges, gullies and canyons, reported in this study are key to advance in the basic knowledge on the geology and geomorphology of the ASAPSC, and have direct implications for future specific research on the characterization of deep ecosystems, geohazards, natural resources, and territory planning.

**Keywords:** submarine geomorphology, SeaFlower Biosphere Reserve, western Caribbean, Roncador Bank, multibeam bathymetry

## INTRODUCTION

The investigation of the seabed geomorphology, i.e., the forms, processes and evolution of submarine landscapes, has become a powerful tool to characterize the renewable and non-renewable marine resources, such as marine ecosystems, fisheries, hydrocarbons, deep sea minerals, among others. Also, knowing the submarine morphology is key to the assessment of geohazards, and to the marine and coastal spatial planning, including the operation of offshore infrastructure, the appointment of protected areas, and the implementation of environmental programs.

The Archipelago of San Andres, Providencia and Santa Catalina (ASAPSC) is located in the western sector of the Caribbean Sea and belongs to the Republic of Colombia (**Figure 1**). This archipelago has an area of 180,000 km<sup>2</sup> approximately (Coralina-Invemar, 2012), and includes the SeaFlower Biosphere Reserve (SBR), one of the most important protected marine areas in the western hemisphere. The ASAPSC comprises two oceanic islands (San Andres and Providencia-Santa Catalina) and a group of atolls and coral banks (Albuquerque, Este-Sureste, Roncador, Quitasueño, Serrana, Serranilla, and Bajo Nuevo, among others), most of which emerge permanently as cays, which support the highest density of corals in the Caribbean Sea. In spite of the well-known importance of the SBR from the biological, ecological and productive point of view, very little is known about its physical aspects, especially on the geological structure and the geomorphological features of the islands and banks in their deep submarine environments.

In this paper, we took advantage of recently acquired multibeam bathymetric information to illuminate and describe, for the very first time, the submarine geomorphology of Roncador Bank, located in the central sector of the ASAPSC. The results presented here are not only important for improving the basic knowledge of the geological and geomorphological origin and evolution of the ASAPSC, but also constitute the basis for carrying out studies of geohazards, mineral resources, and marine ecosystems, and for establishing policies for their exploitation, protection and conservation.

## GEOLOGIC AND OCEANOGRAPHIC CONTEXT OF THE ASAPSC AND RONCADOR BANK

Roncador Bank is located in the ASAPSC, in the northwestern sector of the Colombian Caribbean, approximately 140 km to the east of Providencia Island and 205 km to the northeast of San Andres Island (**Figure 1**). Geologically, the ASAPSC is part of the province known as Lower Nicaraguan Rise (LNR) (Holcombe et al., 1990), which is considered as a crustal block limited by the Pedro Escarpment to the northwest and the Hess Escarpment to the southeast (Holcombe et al., 1990; Mauffret and Leroy, 1997). Case et al. (1990), based on the analysis of multichannel seismic data concluded that the LNR is composed of oceanic crust. Alternatively, Mauffret and Leroy (1997) found that this province is underlain by an oceanic

plateau. Milliman and Supko (1968) superimposed geomagnetic data over the bathymetry in the area of the San Andres Island and found a direct relationship, which is especially pronounced at Este-Sureste atoll. According to these authors, this suggests the presence of deep-seated volcanic cones under the limestone caps of the atolls and of the San Andres Island. The volcanic origin of these formations is further supported by a basaltic pebble that was dredged from a depth of approximately 700 m in the area of the Albuquerque Bank, and by the presence of a prominent platform recognized throughout the area, which can represent the remnants of wave-cut volcanoes, later covered by a thick sediment cover (Milliman and Supko, 1968).

From the few geological studies carried out in the ASAPSC area, it has been concluded that the atolls, islands and coral banks may have originated by volcanic activity during Early Cenozoic times (Geister and Díaz, 2007). In this scenario, subsidence and simultaneous capping of these volcanoes by shallow-water carbonate layers from Cenozoic through Quaternary gave rise to the formation of the shallow banks and atolls of the archipelago (Geister and Díaz, 2007). Most of the banks, atolls and islands of the ASAPSC exhibit a NNE-SSW orientation, suggesting a possible NNE-trending submarine fault zone, which controlled the location of volcanic material on the seafloor. Additionally, the presence of some atolls and elongated islands with a NW-SE trend also suggests the existence of fault zones oriented to the NW underlying these structures.

On the other hand, the geological knowledge of Roncador Bank is quite limited, and what little information is available is restricted to its shallowest part. Roncador is an elongated atoll with an overall NW-SE trend, reaching a maximum amplitude of about 6 km and a length of approximately 13 km (Geister and Díaz, 2007). This bank forms the base of Roncador Cay, a vegetated islet located in the northern sector, formed by the accumulation of coarse coral debris (Geister and Díaz, 2007); its dimensions are 482 m in length and 290 in width (Tabares et al., 2009). The geomorphology of Roncador reef complex has been well characterized by Milliman (1969), and Geister and Díaz (2007). These authors stated that Roncador has a windward fore-reef terrace that is somewhat narrower and deepens more rapidly than that of any of the other ASAPSC atolls. The peripheral reef is continuous only on the windward side (Geister and Díaz, 2007). The lagoon terrace is considerably shallower than that of the other atolls in the area; the depths within the lagoon basin reach approximately 18 m, with an average of 10–12 m (Milliman, 1969; Geister and Díaz, 2007). According to Milliman (1969), the lagoon basin is completely open to the west, with the exception of the southernmost sector, where a few elongated, shallow patch reefs form a discontinuous peripheral reef to the southwest.

The prevailing surface current in the Caribbean Sea, known as the Caribbean Current, is a high-speed flow (>25 cm/s) from E to W, and forms a large counterclockwise eddy in the southwestern sector of the Caribbean (Geister and Díaz, 2007) (**Figure 1**). According to Hallock et al. (1988), the persistent northward flow of this current through large gaps and narrow open seaways of the Nicaraguan Rise is a key oceanographic and environmental factor that controls the sedimentary processes on the western platforms of the rise. The Caribbean Current is

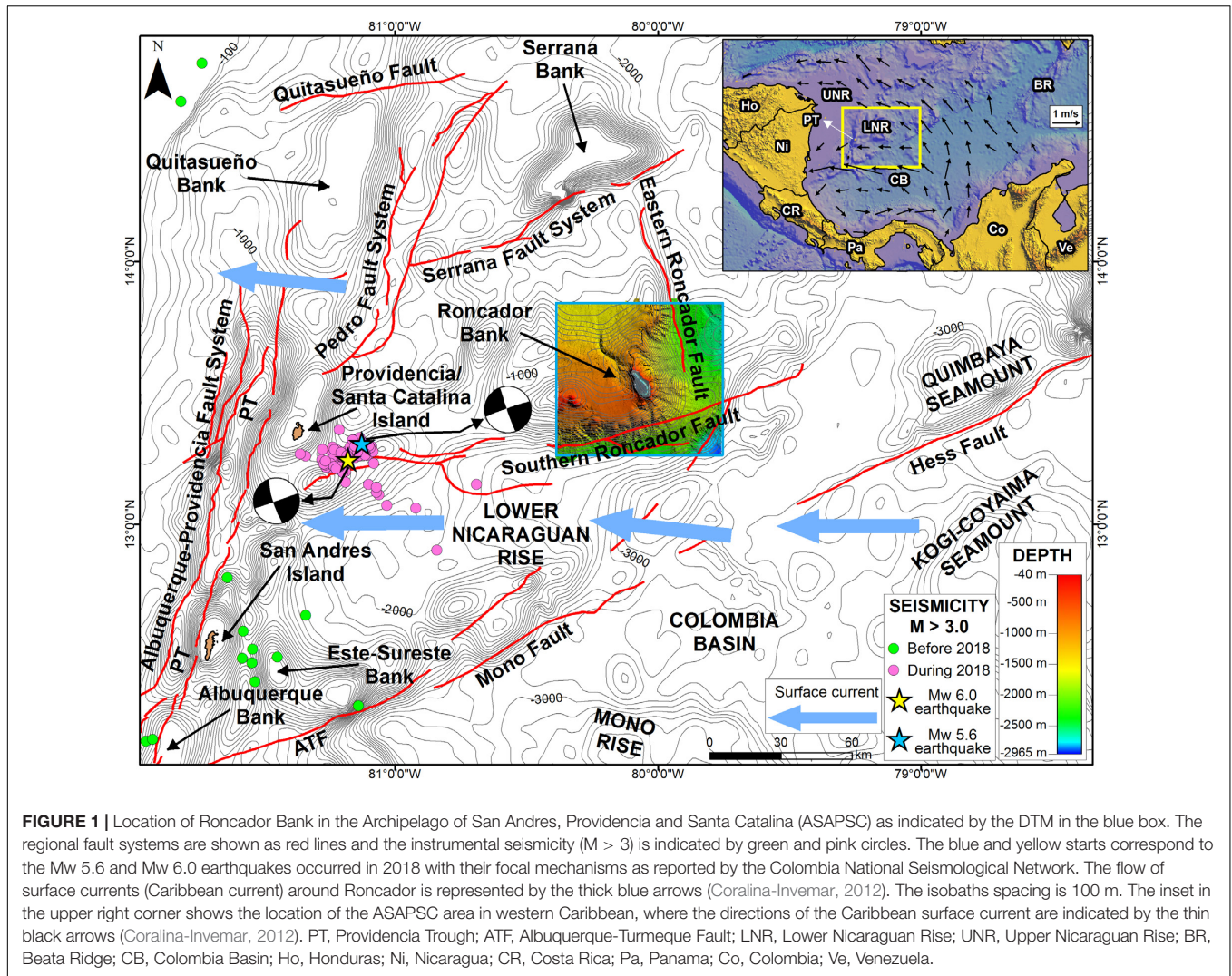


**FIGURE 1 |** Location of Roncador Bank in the Archipelago of San Andres, Providencia and Santa Catalina (ASAPSC) as indicated by the DTM in the blue box. The regional fault systems are shown as red lines and the instrumental seismicity ( $M > 3$ ) is indicated by green and pink circles. The blue and yellow stars correspond to the Mw 5.6 and Mw 6.0 earthquakes occurred in 2018 with their focal mechanisms as reported by the Colombia National Seismological Network. The flow of surface currents (Caribbean current) around Roncador is represented by the thick blue arrows (Coralina-Inveimar, 2012). The isobaths spacing is 100 m. The inset in the upper right corner shows the location of the ASAPSC area in western Caribbean, where the directions of the Caribbean surface current are indicated by the thin black arrows (Coralina-Inveimar, 2012). PT, Providencia Trough; ATF, Albuquerque-Turmeque Fault; LNR, Lower Nicaraguan Rise; UNR, Upper Nicaraguan Rise; BR, Beata Ridge; CB, Colombia Basin; Ho, Honduras; Ni, Nicaragua; CR, Costa Rica; Pa, Panama; Co, Colombia; Ve, Venezuela.

divided just between the islands and cays in such a way that a part (~60%) continues its journey toward the Cayman Sea and the rest recirculates toward the southwestern Caribbean, forming the Colombia-Panama Gyre, whose waters flow to the south of the ASAPSC (Coralina-Inveimar, 2012). The surface currents in the ASAPSC are distorted by the continuous arrival of eddies that rotate in both directions and travel with the Caribbean Current. These eddies are deformed between the walls and escarpments of the archipelago seamounts (Coralina-Inveimar, 2012). According to Coralina-Inveimar (2012), in the archipelago, the Caribbean Surface Water (CSW) reaches a depth between 50 and 75 m and is characterized by its low salinity. A second water mass, the Subtropical Subsurface Water (SSW), with a maximum salinity, is located between 150 and 200 m, followed by a water body known as Subantarctic Intermediate Water (SIW) that has the minimum salinity between 600 and 900 m. Finally, the North Atlantic Deep Water (NADW) is located in the deepest parts of the area. Unfortunately, the behavior of these deep currents (flow directions and velocities) in the ASAPSC area is currently unknown.

## DATA AND METHODS

The acquisition of multibeam bathymetric data in the Roncador area was carried out in 2017 on board the research vessel ARC Malpelo, which is operated by the Center for Oceanographic and Hydrographic Research of Colombia (CIOH), using a Kongsberg EM 302 system with a frequency of 30 kHz. This expedition was part of a huge initiative, led by the General Maritime Directorate of Colombia (DIMAR), to map the entire seabed of the ASAPSC, with the purpose of advancing knowledge of the geology and geomorphology of the Colombian Caribbean underwater environments.

After applying some corrections to the raw depth soundings, a digital terrain model (DTM) was generated with a spatial resolution of 35 m. In order to support our morphological observations and interpretations, we carried out some standard morphometric calculations. These DEM-derived products were obtained using the software ArcGIS 10.3.1, and include the hillshade, slope, aspect, and profile and plan curvature models.



Hillshade is a raster generated from elevation data that provides a shaded surface depending on the angle and azimuth of a hypothetical illumination source, and is typically displayed underneath the transparent bathymetry to enhance visualization of elevation data. The terrain slope is defined as the maximum rate of change in a cell value (elevation) relative to the neighboring cells, and its resulting raster shows the steepest gradient in degrees ranging between 0° (horizontal) and 90° (vertical) (Jenness, 2013). The aspect map shows the azimuth direction at which the maximum slope is achieved (Favalli and Fornaciai, 2017). Since the aspect represents the azimuthal direction of the gravity force component tangential to the surface, generally it is accepted that aspect indicates the flow line direction (Olaya, 2009). The profile curvature is defined as the rate of change of slope measured in a vertical plane oriented along the gradient line (e.g., Olaya, 2009). A negative value indicates convex slopes, while a positive value indicates concave surfaces. Consequently, a value close or equal to zero indicates flat or uniform surfaces. The profile curvature runs parallel to the terrain maximum slope and affects the acceleration or deceleration of flow down the slope (e.g., Wood, 1996; Olaya, 2009; Di Traglia et al., 2014). The planform curvature (commonly called plan curvature) is perpendicular to the direction of the maximum slope. Here, a positive value indicates that the surface is sidewardly convex, and a negative value indicates that the surface is sidewardly concave. A value close or equal to zero indicates flat or uniform surfaces. The plan curvature runs perpendicular to the terrain maximum slope and affects the convergence and divergence of flow down the slope (e.g., Olaya, 2009; Favalli and Fornaciai, 2017).

We also used seafloor backscatter information, which were acquired concurrently with the bathymetry. Our analysis was only qualitative with the aim of evaluating the nature of the substrate, mainly in terms of lithology, roughness and heterogeneities, and to differentiate depositional and erosional areas.

## GENERAL PHYSIOGRAPHY OF RONCADOR BANK

The area covered by the bathymetric survey around Roncador Bank extends between latitudes 13.2° and 13.8°, and longitudes -79.7° and -80.4°, covering about 4,800 km<sup>2</sup>. The information allowed us to determine that the depths in the zone vary between -40 and -2,965 m (Figure 2). The shallowest values (<-2,000 m) are observed in the central and northwestern sectors, whereas deeper values (>-2,000 m) are found to the south and east of the study area (Figure 2). It is also clear that the deep and shallow sectors are separated by a zone of closely spaced isobaths with a general tendency W-E observed at 13.3°N, which exhibits an abrupt direction shift at -80°W to continue with a general tendency N-S (Figure 2). In Figure 3A, this zone shows the steepest slope angles (between 25° and 40°).

The aspect (or slope direction) map allowed us to differentiate four sectors with contrasting characteristics (Figure 3B): the southern sector where slopes oriented within the SE and SW

quadrants (azimuth between 90° and 270°) are predominant; the northeast sector which exhibits slopes oriented mainly to the east, with minor variations to the ENE and ESE; the north-central and southeastern sectors where slopes are oriented preferentially to the NW (average azimuth of 315°); and a northwestern sector which exhibits slopes oriented north and northwest.

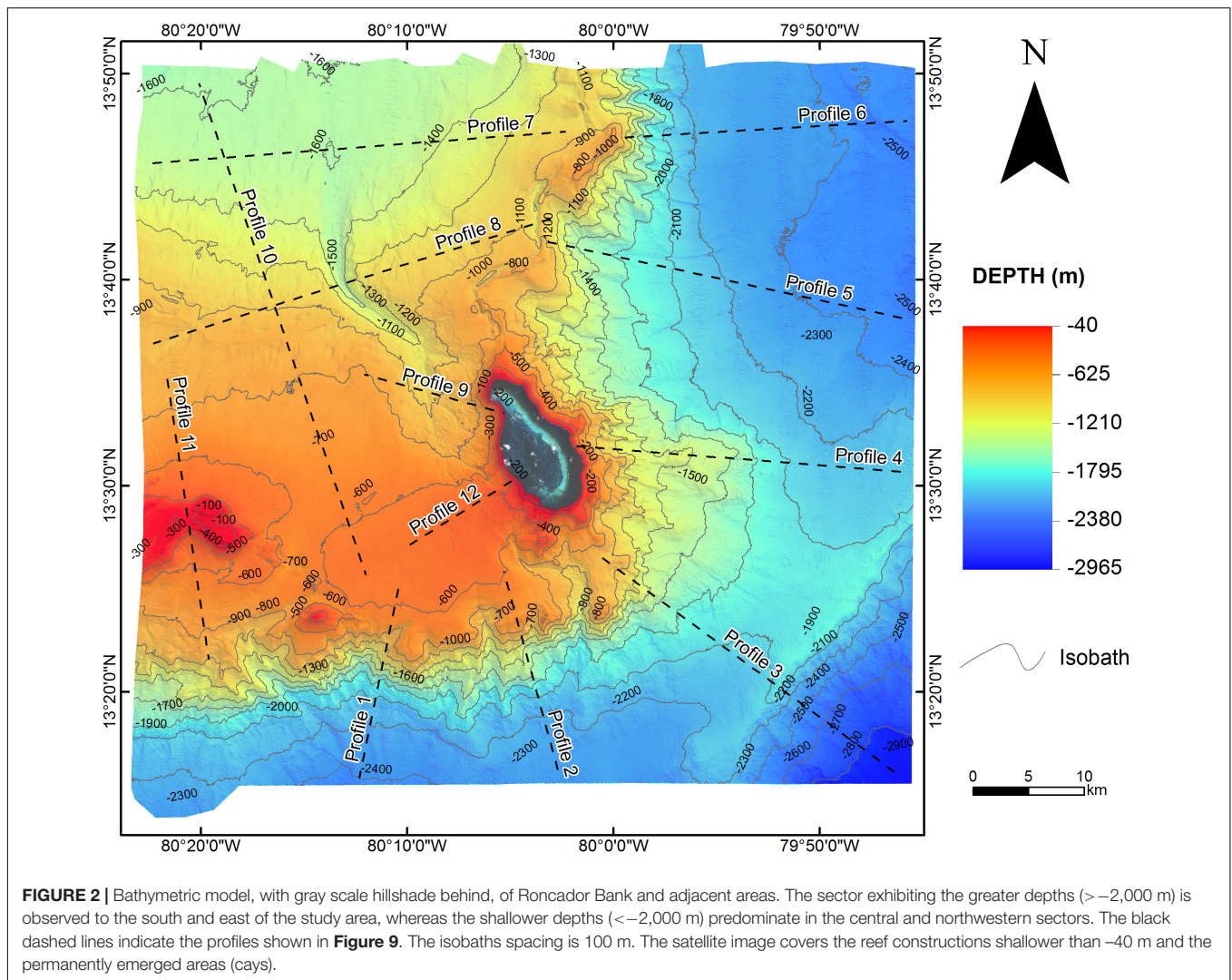
## GEOMORPHOLOGY OF RONCADOR BANK

Morphologically, Roncador corresponds to an irregular-shaped seamount which reaches a maximum height of about 2,350 m with respect to the adjacent relatively flat seafloor. There are several distinct morphologic elements that characterize Roncador Seamount (Figure 4): escarpments; slope deposits; archipelagic apron; pinnacles (volcanic remnants); hummocky terrains; terrain with small-scale scarps and ridges; major ridges; and canyons.

### Escarpments

One of the most prominent geofoms identified in the study area corresponds to a zone of major escarpments, occurring in the southern sector with a general tendency W-E, which suddenly shifts their trend to continue with an S-N direction (Figures 2, 3A-D, 4, 6B,D, 8A,C). These escarpments show steep slopes, with angles varying between 18° and 25°, but locally reaching values of 40°, and oriented toward the SE, SW, ENE, and ESE (Figures 3A,B). One of the most important features of these escarpments is the presence of very complex longitudinal and transverse profiles, as a result of the occurrence of numerous small, narrow and deeply incised gullies (Figures 4, 5A-C, 6B-D, 8A,C, 9A-D). This situation is evident in the profile and plan curvature maps shown in Figures 3C,D, where concave and convex forms are repetitive along the escarpment hillsides. In particular, the profile curvature map of the southern escarpment (Figure 5B) differentiates very well its upper limit, where it is bounded by a relatively regular, gentle sloping surface that extends to the north. The crest of the escarpment is very irregular in plan view; it is evident by an abrupt slope break (Figure 5B) and occurs at depths ranging from -790 to -600 m. In contrast, the lower limit of the escarpment is not so evident in the profile curvature map (Figure 5B). This is due to the fact that the escarpment foothill is partially covered by slope deposits, and therefore the slope change is not as strong as in the escarpment's upper part. On the other hand, the plan curvature map (Figure 5C) clearly delineates the dense gully network present in the southern escarpment. From this map it is evident that the gullies are arranged in a dendritic pattern, and that most of them originate at the slope break that forms the escarpment crest (Figure 5C). Only two gullies have heads extending beyond the upper part of the escarpment, incising the relatively flat surface located to the north (Figures 5A,C). The gullies reach depths up to 300 m beneath the escarpment seafloor. From the backscatter data, shown in Figures 7B-D, it is observed that, in general, the upper part of the escarpments exhibit high reflectivity, being higher in the eastern escarpment,





which implies that volcanic rock and/or limestone crop out there. On the other hand, the middle and lower parts of the escarpments exhibit medium to low reflectivity, implying the presence of softer sea bottom, which is consistent with the occurrence of slope deposits (**Figures 7B–D**).

As is observed in the slope and profile curvatures maps (**Figures 3A,C**), at the top of the eastern escarpment, there is a depression-like feature, slightly sinuous, trending SW–NE. This depression is very narrow (maximum width of 1,000 m), deepens to 200 m below the surrounding seafloor, and reaches a length of about 18 km (**Figures 6A,D**). The backscatter signal of this feature is characterized by high values, indicating a highly reflective seafloor (**Figures 7A,D**). This acoustic response indicates that erosive processes predominate, exposing a hard substrate (volcanic rock and/or limestone), and that sediment cover is scarce or absent.

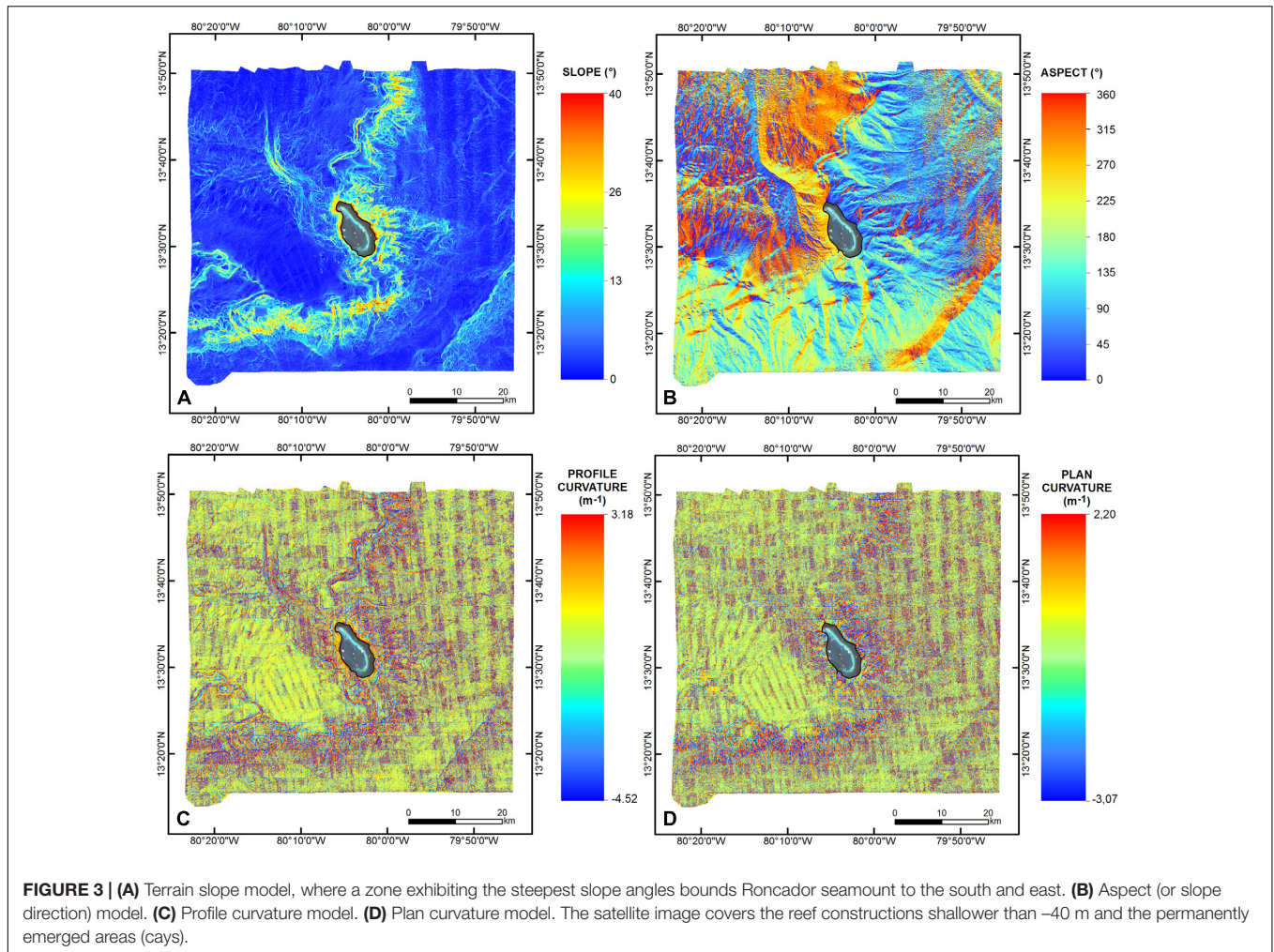
We also infer that Roncador southern and eastern escarpments are tectonically controlled by the activity of two regional faults, named Southern Roncador Fault and Eastern Roncador Fault, respectively. These faults are recognized on

the seafloor as very strong lineaments (**Figures 4, 6B–D**). The Southern Roncador Fault comprises two traces that are oblique to the general direction of the escarpment, and exhibit a strike ranging between  $N72^{\circ}E$  and  $N80^{\circ}E$ ; the Eastern Roncador Fault strikes between  $N5^{\circ}W$  and  $N20^{\circ}W$  (**Figures 4, 6B–D**).

## Slope Deposits

A belt of landforms with low gradients (less than  $8^{\circ}$ ), and geometries of cones and lobes of different sizes and shapes is observed at the foot of the escarpments described above (**Figures 4, 6B–D, 8A,C**). From their morphology, and the fact that they occur at the escarpments foothills, they are interpreted as slope deposits.

Based on the bathymetry data, we were able to differentiate up to 21 individual depositional bodies, which in most cases seem to be bounded by gullies and channels. The individual areas of these deposits vary between 9 and  $138 \text{ km}^2$ , and their surfaces are commonly irregular due to the presence of minor scarps and ridges (**Figures 4, 6B–D, 9A–E,K**). Such textures may have originated as a result of compressional deformation and/or



collapse of the material during the deposition. The backscatter signal shows that the slope deposits have intermediate to low reflectivity, implying that they are mostly composed mostly of fine-grained sediment, with minor quantities of coarser sediment mainly located at their proximal sectors (Figures 7B–D).

### Archipelagic Apron

This geoform is characterized by a very smooth relief, which deepens with a maximum slope of  $5^\circ$ . It is observed in the southeastern and eastern sectors as a relatively flat surface that bounds the slope deposits in deeper areas. Also, it extends from the top of the escarpments to the northwest of the study zone with a gentle slope of about  $3^\circ$  (Figures 4, 6B–D, 8A–D, 9B,D,E,G,J,L). The acoustic reflectivity of the apron surface (Figures 7C,D) is very low, which suggests that this sedimentary body is likely the product of fine-grained, hemipelagic sedimentation, although some bottom current-driven sedimentation should not be discarded.

### Canyon

In the central part of the zone, there is bathymetric expression of a canyon of significant dimensions. This conduit, known

as Roncador Canyon, originates on the western side of the bank, and extends for about 35 km toward the northwest, where it flows into a small fan at a depth of  $-1,580$  m approximately (Figures 4, 6A, 8B,D, 9H,I). The proximal part of this canyon is partially covered by deposits having a hummocky structure (Figures 4, 6A, 8B,D, 9I), inferred to be debris-flow deposits. Roncador Canyon is up to 430 m deep with respect to the adjacent submarine relief, and exhibits a marked V cross section that varies between symmetrical and strongly asymmetric, with canyon walls reaching maximum slope values between  $20^\circ$  and  $35^\circ$  (Figures 3A, 9H,I). The profile curvature map, shown in Figure 3C, delineates very well the canyon margins, and shows that the middle and distal reaches have constant widths, varying between 2.5 and 3 km. By contrast, the proximal reach of the canyon exhibits the largest width, with values between 7.5 and 8.7 km. The thalweg of the Roncador canyon is characterized by a high backscatter signal (Figure 7A), which is evidence that the bottom of the canyon is devoid of sediment. Also, the proximal reach exhibits intermediate values in the seafloor reflectivity (Figure 7A) due to the presence of extensive debris flow deposits, mainly on the eastern hillside.



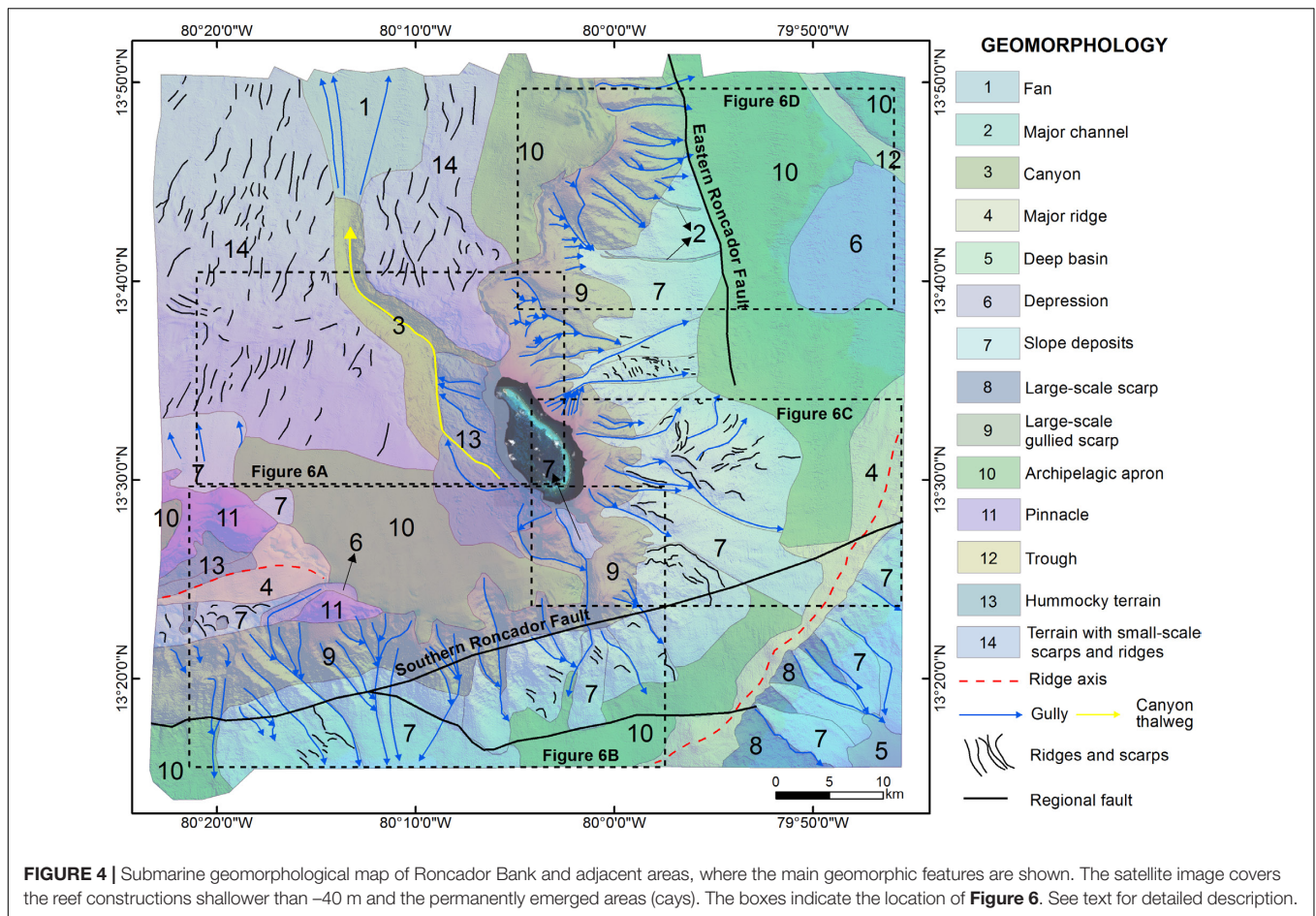


**FIGURE 4 |** Submarine geomorphological map of Roncador Bank and adjacent areas, where the main geomorphic features are shown. The satellite image covers the reef constructions shallower than  $-40$  m and the permanently emerged areas (cays). The boxes indicate the location of **Figure 6**. See text for detailed description.

### Pinnacles

Here, we refer to pinnacles as geofoms associated with cone-shaped elevations mounted on the top of a major submarine feature. We were able to identify two pinnacles in the southwestern sector of the study zone, which are interpreted as remnants of volcanic edifices (**Figures 4, 6B, 8A,B,D, 9K**). This is supported by the backscatter image shown in **Figure 7B**, which provides evidence of a high reflective seafloor associated with these two pinnacles. The pinnacle located to the south rises over the top of the Roncador southern escarpment, reaching a height of 450 m above the surrounding seafloor; its base has a length of about 18.8 km, and its slopes exhibit a complex shape, with both concave and convex profiles. The second pinnacle is located to the northwest of the first pinnacle, and it raises over the archipelagic apron reaching a height of approximately 550 m (**Figures 4, 6B**); its base has a length of about 44 km, and also exhibits an asymmetrical profile, with both concave and convex slopes (**Figure 9K**). Its slopes have an average angle of  $15^\circ$ , but locally can reach up to  $25^\circ$ .

### Hummocky Terrain

This terrain is characterized by a very irregular and rough texture, due to the presence of numerous blocks (or rock fragments) of various sizes deposited on the slopes of major geofoms by

mass wasting processes (**Figures 4, 6A, 8B,D, 9I**). The blocks can reach several tens of meters of height and exhibit very irregular shapes. The most prominent hummocky terrain of the study area is located on the western flank of Roncador seamount, extending to a maximum depth of about  $-1,100$  m, where it appears to be partially filling the proximal reach of the Roncador Canyon eastern wall (**Figures 4, 6A, 8B,D, 9I**). The backscatter signal shows a mixture of intermediate and high reflectivity values (**Figure 7A**). The higher values indicate the blocks or rock fragments, and the intermediate values represent the finer sediment of the deposit. This terrain is interpreted as debris flow deposits produced by a partial collapse of the western margin of Roncador volcanic edifice, and reaches an area of  $93.8 \text{ km}^2$ . Furthermore, a smaller hummocky terrain is observed in the southern part of the northernmost volcanic pinnacle, with an area of approximately  $24 \text{ km}^2$  (**Figures 4, 6B, 7B**).

### Terrain With Small-Scale Ridges and Scarps

In the northwesternmost sector of the study area there is a surface with a general smooth ( $<5^\circ$ ), northward-oriented slope, which exhibits a distinctive irregular relief due to the presence of a series of minor scarps and ridges (**Figures 4, 6A, 8B,D, 9H,J**). These features exhibit a preferential N-NNE strike, although locally



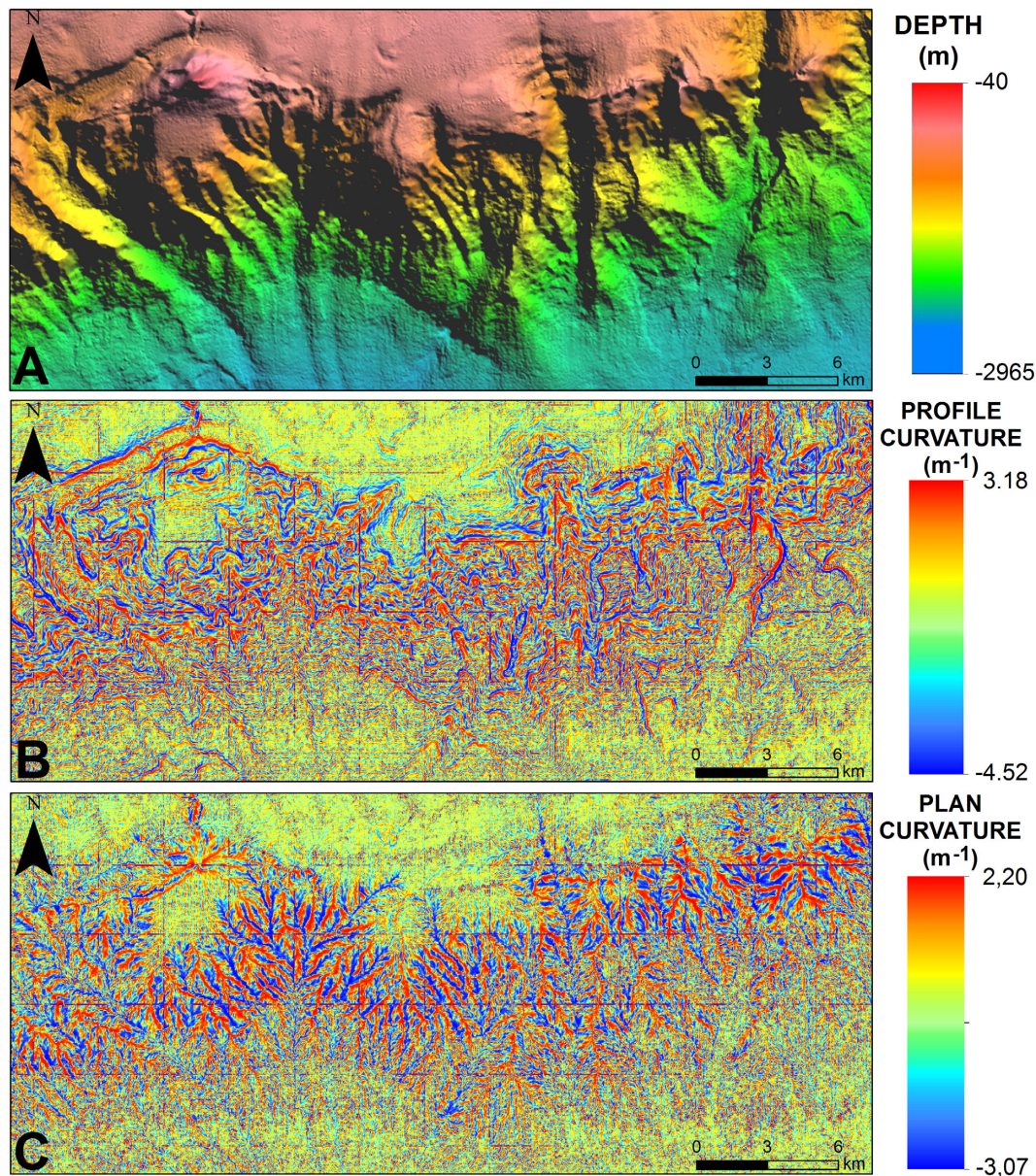


**FIGURE 5** | Detail of Roncador southern escarpment. **(A)** Bathymetric model. **(B)** Profile curvature model. **(C)** Plan curvature model. See text for detailed description.

some are arranged with a general direction E–W (**Figure 3B**). These irregularities can reach maximum heights of several tens of meters above the surrounding seafloor. This terrain occupies about 812 km<sup>2</sup>, but it is important to clarify that this geomorph extends to the north, outside the area covered by this study.

### Major Ridges

In the southeastern sector of the study area, a SW–NE-elongated positive relief is observed, which does not exceed 150 m in height above the surrounding seafloor (**Figures 4, 6C, 8A,C, 9C**). This ridge is bounded to the southeast by an escarpment that extends toward greater depths

outside the study area, and that is partially covered by slope deposits. The ridge presents a strongly asymmetrical cross section with steeper slopes toward the southeast (inclination between 10° and 20°) and smoother slopes to the northwest (inclination < 5°) (**Figures 3A,B**).

### DISCUSSION

According to the few geological and geomorphological studies conducted, it has been proposed that the LNR, the geological province where the ASAPSC is located, is composed of oceanic-type crust, with the peculiarity that it has been affected by intense



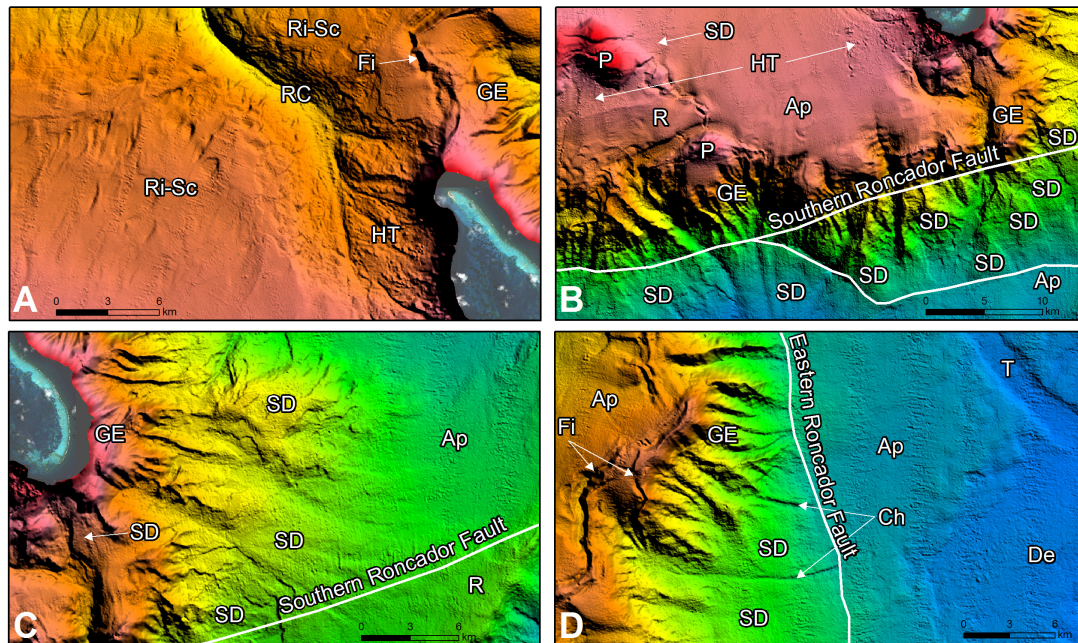


**FIGURE 6** | Detail of some of the most important geoforms associated with Roncador Bank. **(A)** Northwestern sector of Roncador where a hummocky terrain (HT) is identified in the proximal reach of the Roncador Canyon (RC). **(B)** Southern escarpment of Roncador where a series of gullies and slope deposits (SD) are present. This escarpment is controlled by the Southern Roncador Fault. At the top of the escarpment, there are two pinnacles (P). **(C)** Gullied escarpment (GE) in the southeastern sector of Roncador, and extensive slope deposits (SD) at the foothills. **(D)** Eastern escarpment of Roncador which is controlled by the Eastern Roncador Fault. At the top of the escarpment, a fissure (Fi) is identified. The satellite image covers the reef constructions shallower than  $-40$  m and the permanently emerged areas (cays). Ri-Sc, terrain with minor ridges and scarps corresponding to large-scale landslides deposits; R, ridge; Ap, archipelagic apron; De, depression; T, trough; Ch, channel. See **Figure 4** for location.

volcanism since Cenozoic times. In this sense, Geister (1992) and Geister and Díaz (2007) reported the common presence of geological features such as seamounts and volcanoes with a preferential NE–SW orientation. Additionally, on Providencia Island, volcanic rocks crop out, including basalts and trachytes (Mitchell, 1955; Wadge and Wooden, 1982; Geister, 1992). Although from the middle of the last century it has been known that the islands, atolls and banks that make up the ASAPSC lie on a basement of volcanic origin, very little is known about the geomorphological features that these formations exhibit in the deep environments, beyond the outer limit of shallower reef constructions. In this work, we contribute to the advance of the geological knowledge of the ASAPSC, by means of the detailed geomorphological description of Roncador Bank from newly acquired multibeam bathymetric data.

Our analysis allowed us to identify and map a series of geomorphological features in the Roncador Bank area, which are the product of volcanic, erosive and depositional processes that have interacted during the geological history of the bank. Roncador corresponds to a seamount, which is one of the several volcanic edifices that make up the ASAPSC. This seamount is limited to the south and east by two escarpments, with general directions E–W and N–S, respectively, which are controlled tectonically by two regional faults: Southern Roncador Fault and Eastern Roncador Fault. Two facts lead us to affirm that these two faults are probably active. The first is that both structures

are recognized in the bathymetry as strong lineaments, even when they go through the slope deposits and sedimentary apron. Thus, the faults seem not to be buried by the most recent sedimentation. However, as an alternative, this situation could be the consequence of a very low sedimentation rate in the area, i.e., there is not enough sediment to bury the faults since their last activity, or perhaps bottom currents remove any sediment that is being deposited. The second fact is that although in the Roncador area itself there is no recorded seismicity, the Southern Roncador Fault to the west of the analyzed zone does have earthquake activity (**Figure 1**). During October and November 2018, a seismic swarm of more than 400 earthquakes occurred, the largest at magnitude 6.0, as reported by the Colombia National Seismological Network (CNSN). The focal mechanisms obtained by the CNSN for the Mw 6.0 earthquake and a Mw 5.6 aftershock indicate left-lateral faulting, which is consistent with the Caribbean intraplate strike-slip tectonics previously reported by several authors (Burke et al., 1984; Mann and Burke, 1984; Carvajal-Arenas and Mann, 2018). Such activity not only proves the active character of the Southern Roncador Fault but recognizes its seismogenic potential, and therefore the implication for the seismic risk in the ASAPSC.

The presence of currently active faults supports the hypothesis previously raised by some authors (e.g., Geister, 1992; Geister and Díaz, 2007) that the construction of the ASAPSC volcanic edifices was strongly controlled by regional tectonic structures. In

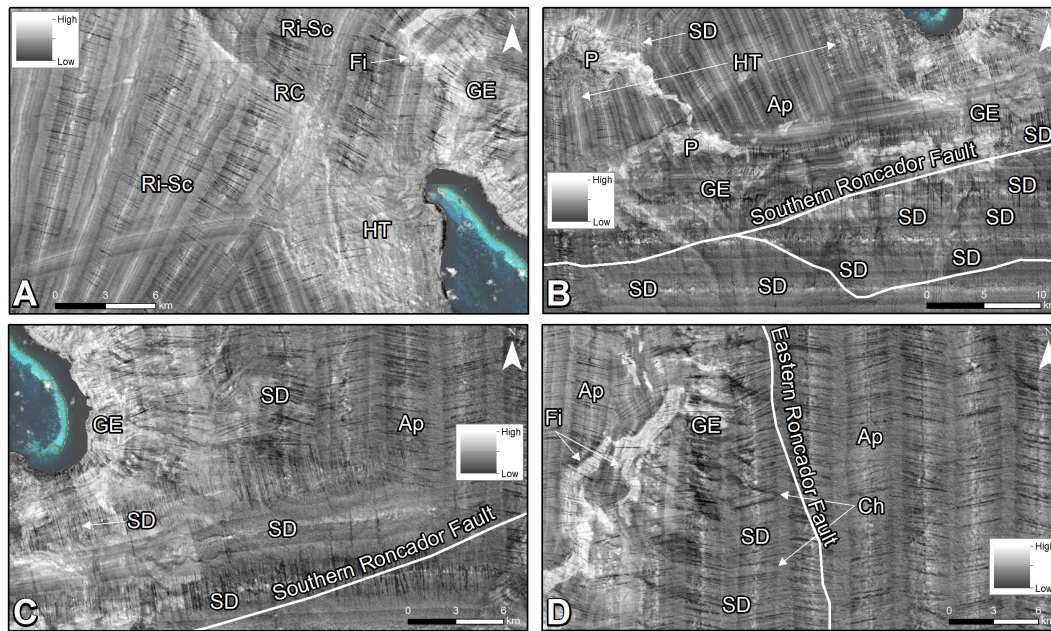


**FIGURE 7 |** Backscatter signal of the seafloor in the same sector shown in **Figure 6**. **(A)** In the northwestern sector of Roncador, the hummocky terrain (HT) is characterized by a mixture of intermediate and high values of seafloor reflectivity. The thalweg of Roncador Canyon (RC), the gullied escarpment (GE) and the fissure (Fi) exhibit high backscatter values. **(B)** Southern escarpment of Roncador where the slope deposits (SD) show low backscatter signal, demonstrating their depositional character. The two pinnacles (P) at the top of the escarpment exhibit high values of reflectivity. **(C)** Gullied escarpment (GE) in the southeastern sector of Roncador characterized by very high backscatter, and extensive slope deposits (SD) at the foothills exhibiting intermediate to low acoustic reflectivity. **(D)** A fissure (Fi) at the top of the eastern escarpment of Roncador is evident by very high backscatter values. The satellite image covers the reef constructions shallower than -40 m and the permanently emerged areas (cays). Ri-SC, terrain with minor ridges and scarps corresponding to large-scale landslides deposits; Ap, archipelagic apron; Ch, channel. See **Figure 4** for location.

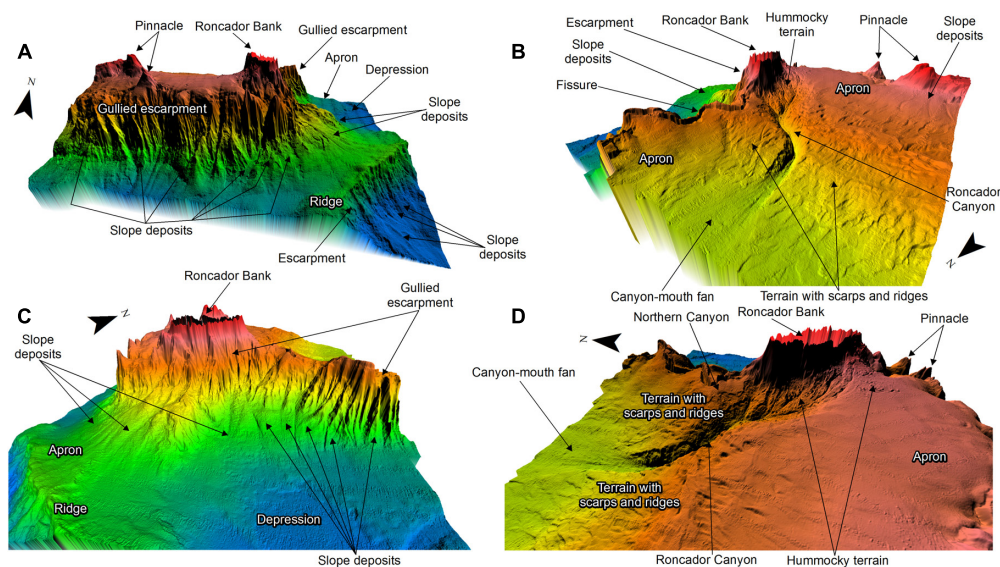


**FIGURE 8 |** General 3D views of Roncador Bank and adjacent areas where the main identified geoforms are highlighted. **(A)** View from the south. **(B)** View from the northwest. **(C)** View from the east. **(D)** View from the west. Vertical exaggeration is by 8. See text for detailed description.

this sense, the Roncador seamount was built by the accumulation of volcanic material on the seabed, which took advantage of the presence of large fractures (Southern and Eastern Faults)

to penetrate the oceanic crust and extrude to the surface. The narrow and deep depression identified in the northern sector of Roncador, along the top of the eastern escarpment, probably



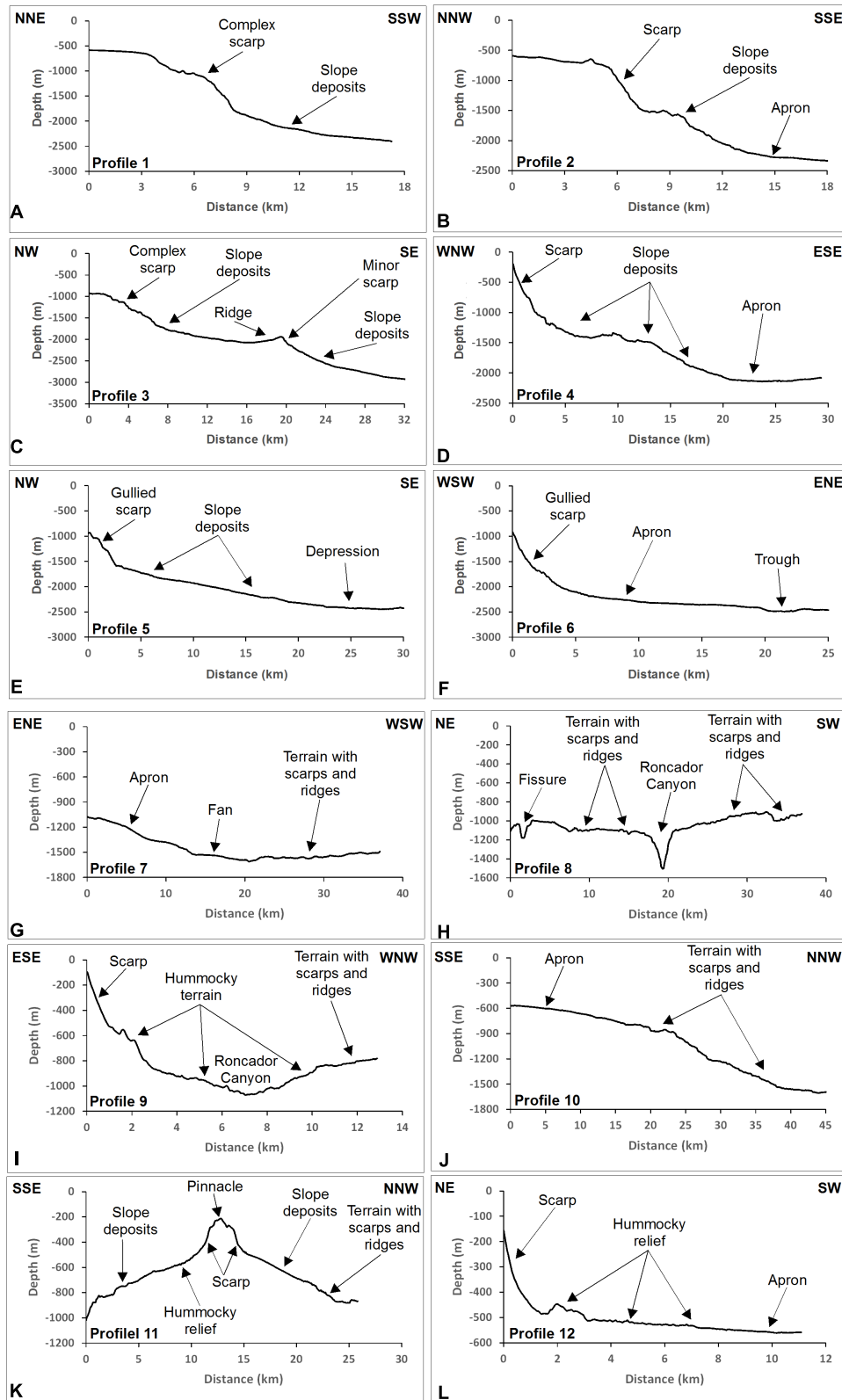


**FIGURE 9 |** Bathymetric profiles showing the main geomorphological features of Roncador Bank and adjacent areas. (A–C) Southern escarpment. (D–F) Eastern escarpment. (G–I) Northwestern sector. (J–L) Western sector. See Figure 2 for the profiles location.

corresponds to a volcanic fissure, that is, a fracture filled by volcanic material.

On the other hand, the presence of a series of embayments along the upper flanks and a belt of slope deposits along the lower parts of the escarpments provide evidence that erosion and sedimentation processes have been important in the evolution of the Roncador volcanic edifice. In fact, erosive processes seem to prevail over the upper and middle parts of the Roncador escarpments, which in consequence results in active supplying of sediments downslope. Some authors have suggested that the overall slope geometry relates to the underlying lithology and to the prevailing sediment transport mechanisms (e.g., Adams et al., 1998; Adams and Schlager, 2000). For example, Adams and Kenter (2014) established that concave slope profiles are common in carbonate settings, as this type of lithology tends to build steeper slopes than their siliciclastic counterparts. The observation of some concave profiles in both southern and eastern escarpments of Roncador (**Figures 9B,D,F,I,L**), in association with the presence of steep slopes and high to intermediate backscatter intensities, indicates that the upper flanks are predominantly made of hard substrate, limestone and/or volcanic rock. Also, some bathymetric profiles clearly show the change from a zone exhibiting concave, steep slopes to a zone showing convex, gentler slopes or, in some cases, alternating concave-convex slopes (**Figures 9B,D,L**). This marks the transition from an erosive regime in the upper part of the escarpments to a depositional regime toward the seamount base. The steep slopes of the escarpments (up to 40°) favors the concentration of mass wasting processes, which is evident by the occurrence of a dense network of gullies parallel to the slope. These gullies serve as conduits for the sedimentary material that moves from the shallower parts to the foot of the seamount, where it is deposited forming sediment bodies in the form of lobes and cones.

Development and survival of submarine canyons rely on the availability of a proximal source of sediment, and appropriate sediment transport mechanisms, such as ocean currents and mass wasting (Normandeau et al., 2014; Puig et al., 2014). We have determined that the Roncador Canyon originates on the northwestern flank of Roncador edifice and runs to the northwest for approximately 35 km. Therefore, the proximal and direct sediment source for the canyon is the western slope of the seamount and atoll rim, which implies that downslope erosive flows have played a role in the canyon evolution. The canyon upper reach is covered by an extensive debris-avalanche deposit, recognized by its typical hummocky morphology. This deposit is incised by a series of gullies which flow into the Roncador Canyon. From our analysis, we were able to infer that Roncador western flank have been, and likely are actively providing sediments downslope to Roncador Canyon, by means of the gullies, which act as channels funneling sediment from the upper parts of the atoll toward the canyon. Two facts further support this hypothesis. First, the high backscatter intensities observed along the gullies and the canyon thalweg (**Figure 7A**), implying that these conduits are sediment starved. Second, the presence of a fan in the canyon mouth (**Figures 8B,D**), produced by deposition of the sediment transported through the gullies

and canyon. Roncador Canyon and its feeder gullies, as well as the gully networks present in the southern and eastern escarpments of Roncador edifice originated from gravity flows whose source could be mass wasting processes and/or cascading, dense-water flows. The first is supported by the common observation of slide scars in the heads of gullies and canyons. The presence of several water masses in the Roncador area, the CSW up to 50–75 m depth and the SSW between 150 and 200 m (Coralina-Invenmar, 2012), accounts for the possibility of dense-water flows. The depth range of the transition between these two water masses is very similar to the depth of the atoll outer rim where the shelf-break is located. Several works have reported the strong influence of dense water cascades-triggered gravity flows in the formation and evolution of gullies and canyons (e.g., Canals et al., 2006; Micallef and Mountjoy, 2011).

It is widely established from numerous studies (e.g., Rebesco et al., 2014; Ercilla et al., 2016) that bottom currents strongly shape the seafloor through erosion, transport and deposition. In the ASAPSC area, Coralina-Invenmar (2012) has reported the existence of at least four water masses: CSW, SSW, SIW, and NADW. Although the depth ranges to which these water bodies extend are relatively well constrained, their present-day circulation patterns (directions and velocities) have not yet been measured, particularly the deeper flows, such as SIW and NADW. Thus, it is necessary to undertake physical oceanography studies to characterize the dynamic behavior of deep water flows in order to establish the significance of bottom current processes in shaping the ASAPSC deep-sea morphology. Having in mind that water masses that circulate in modern oceans and seas are able to transport sediment over long distances, and their bottom component can re-suspend and advect eroded seafloor (Ercilla et al., 2016), the link between the ASAPSC deep currents and some morphological features described in Roncador area (such as escarpments, sedimentary aprons, canyons and gullies, among others) should be addressed.

It is well known that seamounts or volcanic islands are highly susceptible to partial collapses of their edifices, mainly due to the high slope gradients, intense fracturing, chemical weathering associated with volcanic processes, earthquake activity, among other causes (Fairbridge, 1950; Ui, 1983; Siebert, 1984). Commonly, this type of collapse produces debris avalanches, whose deposits typically exhibit hummocky morphology (e.g., Moore et al., 1989; Le Friant et al., 2009). In this study, we identified a terrain with hummocky structure located in the western sector of Roncador, evidence of a partial collapse of that sector of the seamount. Geister and Díaz (2007) reported that the Roncador western platform margin is formed by an almost continuous vertical to overhanging cliff plunging from an 18 m deep shelf-edge into the ocean, which appears to have formed by break-off of the outer shelf margins. Here, the atoll rim is characterized by a major arcuate bight-like geometry, widely recognized as the morphological expression of large submarine failures (Fairbridge, 1950; Terry and Goff, 2013).

In contrast to the Roncador southern and eastern flanks, which are limited by large escarpments, toward the northwestern sector the seamount extends through a relatively gentle surface with irregular relief due to the presence of multiple minor

scarp and ridges. This terrain could correspond to an extensive sedimentary deposit product of the collapse of the Roncador northwestern flank, where the scarps and ridges may represent deformational structures generated at the moment of the material deposition. Detailed studies are necessary to confirm or refute this hypothesis.

Regarding potential geohazards, the recognition of a partial collapse event of the Roncador volcanic edifice implies the possible occurrence of landslide-triggered tsunamis in the geological past. This hypothesis is further supported by the presence of very large limestone boulders on the Roncador western outer reef flat, which must have been deposited by extremely high-energy events, such as tsunamis, although storm surges should not be discarded. Other platform margin failures, evidenced by a series of steep escarpments, have been identified in the southeastern sector of San Andres Island, the northwestern sector of Providencia Island, and the western flank of Serrana bank (Geister and Díaz, 2007). For all these previous cases, Idárraga-García et al. (under review) identified the corresponding landslide deposits in the deeper marine areas. The occurrence of a tsunami event today could have an important impact on the neighboring and densely populated islands of San Andres, Providencia and Santa Catalina, so it is very important to promote detailed analysis of the tsunamigenic potential in the area, related mainly to underwater landslide events.

According to Rogers (1994), seamounts have been thought to play an important role in patterns of marine biogeography, support high biodiversity and host unique biological communities. Differences in seamount seabed morphology influence hydrodynamic flow patterns and therefore the deposition of sediment and organic matter (Clark et al., 2010). In Roncador, we have determined that the seamount is limited to the south and east by two escarpments, which exhibit steep slopes (between 18° and 25°, locally reaching 40°) that are mostly bare rock. The same characteristics are shared by the two volcanic pinnacles located to the southwest of the study zone. There is growing evidence that submarine features exhibiting abrupt slope angles host a variety of species assemblages as well as high abundances of certain species of cold-water corals (Huvenne et al., 2011; Robert et al., 2015, 2017). This situation has an effect in the distribution and abundance of benthic and sessile fauna in Roncador, and it is an issue that must be studied in detail, since at present there is no research that addresses the close relationship between geomorphology and the biological communities in the SeaFlower zone, at least in its deep environments.

Also, in this work we reported and described in detail some other morphologic features which have important implications on future biodiversity and ecosystem research in the archipelago. For example, the Roncador Canyon, which runs for approximately 35 km and exhibits maximum widths of 8.7 km and depths of 430 m beneath the surrounding seafloor. It is well known that unusual physical oceanographic conditions inside submarine canyons increase suspended particulate matter concentrations and transport of organic matter from coastal zones to the deep ocean (Bosley et al., 2004; Genin, 2004; Canals et al., 2006). These processes are responsible for enhancing both pelagic and benthic productivity inside canyon habitats as

well as biodiversity of many benthic faunal groups (Rowe et al., 1982; Vetter et al., 2010). Also, there is increasing evidence of how canyons benefit and support fisheries (Yoklavich et al., 2000), enhance carbon sequestration and storage (Epping et al., 2002; Canals et al., 2006; Masson et al., 2010), provide nursery and refuge sites for other marine life, including vulnerable ecosystems and essential fish-habitats such as cold-water corals and sponge fields (De Leo et al., 2010; Fernandez-Arcaya et al., 2013; Davies et al., 2014). Therefore, the Roncador Canyon should be considered as a geomorphological feature of primary interest to establish its influence on the circulation patterns of deep sea currents, and consequently its relationship with the presence of certain types of ecosystems.

## CONCLUSION

The analysis of high-resolution bathymetric information acquired recently in the SBR (Archipelago of San Andres, Providencia and Santa Catalina) allowed us to describe in detail the underwater morphology of Roncador Bank and adjacent areas. The results obtained in this study support the volcanic origin of the Roncador seamount and the influence of faults (e.g., Roncador Southern Fault and Roncador Eastern Fault) on the ocean floor that acted as zones of weakness that allowed the volcanic material to penetrate the oceanic crust and reach the surface. We suggest that these faults are probably active and therefore seismogenic potential that must be analyzed in order to better assess the seismic risk for the ASAPSC. Also, we were able to determine that erosion and sedimentation processes have played an important role in the evolution of Roncador area. Debris-avalanche deposits were identified as a result of partial collapses of the volcanic edifice. Such mass-wasting has not only acted as shaping agents for the seamount morphology, but also as potential generators of tsunamis in the geological past. Due to this, detailed studies must be carried out to advance the knowledge of geohazards due to landslide-related tsunamis.

Finally, the results presented here contribute significantly to the basic knowledge of the geology and geomorphology of Roncador and adjacent areas, with direct applications in ecosystem characterization, geohazards assessment, and territory management.

## AUTHOR CONTRIBUTIONS

HL carried out the pre-processing of the raw multibeam data and prepared the DTMs. He also contributed to the preparation of the manuscript. JI-G carried out the geological interpretation of the bathymetric data and prepared the figures and the manuscript.

## FUNDING

This study was funded by the Administrative Department of Science, Technology and Innovation of Colombia (COLCIENCIAS) by means of the National Program for Financing Science, Technology and Innovation “Francisco



José de Caldas” and “Colombia BIO” project. JI-G thanks COLCIENCIAS for funding his postdoctoral position at the Oceanographic and Hydrographic Research Center of Colombia (CIOH).

## ACKNOWLEDGMENTS

This research was developed within the framework of the National Plan for Scientific Expeditions “SeaFlower.”

## REFERENCES

- Adams, E. W., and Kenter, J. A. (2014). So different, yet so similar: comparing and contrasting siliciclastic and carbonate slopes. Deposits, architecture and controls of carbonate margin, slope and basinal settings. *SEPM Spec. Publ.* 105, 14–25.
- Adams, E. W., and Schlager, W. (2000). Basic types of submarine slope curvature. *J. Sediment. Res.* 70, 814–828. doi: 10.1306/2DC4093A-0E47-11D7-8643000102C1865D
- Adams, E. W., Schlager, W., and Wattel, E. (1998). Submarine slopes with an exponential curvature. *Sediment. Geol.* 117, 135–141. doi: 10.1016/S0037-0738(98)00044-X
- Bosley, K. L., Lavelle, J. W., Brodeur, R. D., Wakefield, W. W., Emmett, R. L., Baker, E. T., et al. (2004). Biological and physical processes in and around Astoria Submarine Canyon, Oregon, USA. *J. Mar. Syst.* 50, 21–37. doi: 10.1016/j.jmarsys.2003.06.006
- Burke, K., Cooper, C., Dewey, J. F., Mann, P., and Pindell, J. L. (1984). Caribbean tectonics and relative plate motions. *Geol. Soc. Am. Bull.* 162, 31–63. doi: 10.1130/MEM162-p31
- Canals, M., Puig, P., Durrieu de Madron, X., Heussner, S., Palanques, A., and Fabres, J. (2006). Flushing submarine canyons. *Nature* 444, 354–357. doi: 10.1038/nature05271
- Carvajal-Arenas, L. C., and Mann, P. (2018). Western Caribbean intraplate deformation: defining a continuous and active microplate boundary along the San Andres rift and Hess Escarpment fault zone, Colombian Caribbean Sea. *AAPG Bull.* 102, 1523–1563. doi: 10.1306/12081717221
- Case, J. E., MacDonald, W. D., and Fox, P. J. (1990). “Caribbean crustal provinces: seismic and gravity evidence,” in *The Geology of North America*, Vol. H, eds G. Dengo and J. E. Case (Boulder, CO: The Geological Society of America), 15–36.
- Clark, M. R., Rowden, A. A., Schlacher, T., Williams, A., Consalvey, M., Stocks, K. L., et al. (2010). The ecology of seamounts: structure, function, and human impacts. *Ann. Rev. Mar. Sci.* 2, 253–278. doi: 10.1146/annurev-marine-120308-081109
- Coralina-Invemar (2012). *Atlas De La Reserva De Biósfera SeaFlower. Archipiélago De San Andrés, Providencia Y Santa Catalina. Instituto De Investigaciones Marinas Y Costeras “José Benito Vives De Andrés” INVEMAR- Y Corporación para el Desarrollo Sostenible Del Archipiélago De San Andrés, Providencia Y Santa Catalina -CORALINA-. Serie De Publicaciones Especiales De INVEMAR # 28.* Colombia: Santa Marta, 180.
- Davies, J. S., Howell, K. L., Stewart, H. A., Guinan, J., and Golding, N. (2014). Defining biological assemblages (biotopes) of conservation interest in the submarine canyons of the south west approaches (offshore United Kingdom) for use in marine habitat mapping. *Deep Sea Res. II Top. Stud. Oceanogr.* 104, 208–229. doi: 10.1016/j.dsr2.2014.02.001
- De Leo, F. C., Smith, C. R., Rowden, A. A., Bowden, D. A., and Clark, M. R. (2010). Submarine canyons: hotspots of benthic biomass and productivity in the deep sea. *Proc. R. Soc. Lond. B Biol. Sci.* 277, 2783–2792. doi: 10.1098/rspb.2010.0462
- Di Traglia, F., Morelli, S., Casagli, N., and Garduño Monroy, V. H. (2014). Semi-automatic delimitation of volcanic edifice boundaries: validation and application to the cinder cones of the Tancitaro-Nueva Italia region (Michoacán-Guanajuato Volcanic Field, Mexico). *Geomorphology* 219, 152–160. doi: 10.1016/j.geomorph.2014.05.002
- Epping, E., van der Zee, C., Soetaert, K., and Helder, W. (2002). On the oxidation and burial of organic carbon in sediments of the Iberian margin and Nazaré Canyon (NE Atlantic). *Prog. Oceanogr.* 52, 399–431. doi: 10.1016/S0079-6611(02)00017-4
- Ercilla, G., Juan, C., Hernández-Molina, F. J., Bruno, M., Estrada, F., Alonso, B., et al. (2016). Significance of bottom currents in deep-sea morphodynamics: an example from the Alboran Sea. *Mar. Geol.* 378, 157–170. doi: 10.1016/j.margeo.2015.09.007
- Fairbridge, R. W. (1950). Landslide patterns on oceanic volcanoes and atolls. *Geog. J.* 45, 84–88. doi: 10.2307/1789022
- Favalli, M., and Fornaciai, A. (2017). Visualization and comparison of DEM-derived parameters. application to volcanic areas. *Geomorphology* 290, 69–84. doi:10.1016/j.geomorph.2017.02.029
- Fernandez-Arcaya, U., Rotllant, G., Ramirez-Llodra, E., Recasens, L., Aguzzi, J., and Flexas, M. D. M. (2013). Reproductive biology and recruitment of the deep-sea fish community from the NW Mediterranean continental margin. *Prog. Oceanogr.* 118, 222–234. doi: 10.1016/j.pocean.2013.07.019
- Geister, J. (1992). Modern reef development and Cenozoic evolution of an oceanic island/reef complex: isla de Providencia (western Caribbean Sea, Colombia). *Facies* 27, 1–69. doi: 10.1007/BF02536804
- Geister, J., and Díaz, J. M. (2007). *Reef Environments and Geology of an Oceanic Archipelago: San Andres, Old Providence and Sta. Catalina (Caribbean Sea, Colombia)*. Colombia: Boletín Geológico Instituto Nacional de Investigaciones Geológico Mineras de, 142.
- Genin, A. (2004). Bio-physical coupling in the formation of zooplankton and fish aggregations over abrupt topographies. *J. Mar. Syst.* 50, 3–20. doi: 10.1016/j.jmarsys.2003.10.008
- Hallock, P., Hine, A. C., Vargo, G. A., Elrod, J. A., and Jaap, W. C. (1988). Platforms of the nicaraguan rise: examples of the sensitivity of carbonate sedimentation to excess trophic resources. *Geology* 16, 1104–1107. doi: 10.1130/0091-7613(1988)016<1104:POTNRE>2.3.CO;2
- Holcombe, T. L., Ladd, J. W., Westbrook, G., Edgar, N. T., and Bowland, C. L. (1990). “Caribbean marine geology: ridges and basins of the plate interior,” in *The Geology of North America*, Vol. H, eds G. Dengo and J. E. Case (Boulder, CO: The Geological Society of America: ), 231–306.
- Huvenne, V. A. I., Tyler, P. A., Masson, D. G., Fisher, E. H., Hauton, C., Hühnerbach, V., et al. (2011). A picture on the wall: innovative mapping reveals cold-water coral refuge in submarine canyon. *PLoS One* 6:e28755. doi: 10.1371/journal.pone.0028755
- Jenness, J. (2013). *DEM Surface Tools for ArcGIS (Version 2.1.399)*. Available at: [http://www.jennessent.com/arcgis/surface\\_area.htm](http://www.jennessent.com/arcgis/surface_area.htm)
- Le Friant, A., Boudon, G., Arnulf, A., and Robertson, R. E. A. (2009). Debris avalanche deposits offshore St. Vincent (West Indies): impact of flank-collapse events on the morphological evolution of the island. *J. Volcanol. Geotherm. Res.* 179, 1–10. doi: 10.1016/j.jvolgeores.2008.09.022
- Mann, P., and Burke, K. (1984). Neotectonics of the Caribbean. *Rev. Geophys. Space Phys.* 22, 309–362. doi: 10.1029/RG022i004p0309
- Masson, D. G., Huvenne, V. A. I., de Stigter, H. C., Wolff, G. A., Kiriakoulakis, K., and Arzola, R. G. (2010). Efficient burial of carbon in a submarine canyon. *Geology* 38, 831–834. doi: 10.1130/G30895.1
- Mauffret, A., and Leroy, S. M. (1997). Seismic stratigraphy and structure of the Caribbean igneous province. *Tectonophysics* 283, 61–104. doi: 10.1016/S0040-1951(97)00103-0
- Micallef, A., and Mountjoy, J. J. (2011). A topographic signature of a hydrodynamic origin for submarine gullies. *Geology* 39, 115–118. doi: 10.1130/G31475.1

- Milliman, J. D. (1969). Four southwestern caribbean atolls: courtown cays, albuquerque cays, roncadador bank and serrana bank. *Atoll Res. Bull.* 129, 1–26. doi: 10.5479/si.00775630.129.1
- Milliman, J. D., and Supko, P. R. (1968). On the geology of san andres island, western caribbean. *Geol. En Mijnbouw* 47, 102–105.
- Mitchell, R. C. (1955). Geologic and petrographic notes on the colombian islands of la providencia and san andres, west indies. *Geol. En Mijnbouw* 17, 76–83.
- Moore, J. G., Clague, D. A., Holcomb, R. T., Lipman, P. W., Normark, W. R., and Torresan, M. E. (1989). Prodigious submarine landslides on the hawaiian ridge. *J. Geophys. Res.* 94, 17465–17484. doi: 10.1029/JB094iB12p17465
- Normandeau, A., Lajeunesse, P., St-Onge, G., Bourgault, D., Drouin, S. S.-O., Senneville, S., et al. (2014). Morphodynamics in sediment-starved inner-shelf submarine canyons (Lower St. Lawrence Estuary, Eastern Canada). *Mar. Geol.* 357, 243–255. doi: 10.1016/j.margeo.2014.08.012
- Olaya, V. (2009). “Basic land-surface parameters,” in *Geomorphometry: Concepts, Software, Applications, Developments in Soil Science*, eds T. Hengl and H. I. Reuter (Amsterdam: Elsevier), 141–169.
- Puig, P., Palanques, A., and Martín, J. (2014). Contemporary sediment-transport processes in submarine canyons. *Annu. Rev. Mar. Sci.* 6, 53–77. doi: 10.1146/annurev-marine-010213-135037
- Rebesco, M., Hernández-Molina, J., van Rooij, D., and Wählin, A. (2014). Contourites and associated sediments controlled by deep-water circulation processes: state-of-the-art and future considerations. *Mar. Geol.* 352, 111–154. doi: 10.1016/j.margeo.2014.03.011
- Robert, K., Huvenne, V. A. I., Georgiopolou, A., Jones, D. O. B., Marsh, L., Carter, G. D. O., et al. (2017). New approaches to high-resolution mapping of marine vertical structures. *Sci. Rep.* 7:9005. doi: 10.1038/s41598-017-09382-z
- Robert, K., Jones, D. O. B., Tyler, P. A., Van Rooij, D., and Huvenne, V. A. I. (2015). Finding the hotspots within a biodiversity hotspot: finescale biological predictions within a submarine canyon using high-resolution acoustic mapping techniques. *Mar. Ecol.* 36, 1256–1276. doi: 10.1111/maec.12228
- Rogers, A. D. (1994). The biology of seamounts. *Adv. Mar. Biol.* 30, 305–351. doi: 10.1016/S0065-2881(08)60065-6
- Rowe, G. T., Polloni, P. T., and Haedrich, R. L. (1982). The deep-sea macrobenthos on the continental margin of the Northwest Atlantic Ocean. *Deep Sea Res.* A 29, 257–278. doi: 10.1016/0198-0149(82)90113-3
- Siebert, L. (1984). Large volcanic debris avalanches: characteristics of source areas, deposits, and associated eruptions. *J. Volcanol. Geotherm. Res.* 22, 163–197. doi: 10.1016/0377-0273(84)90002-7
- Tabares, N., Soltan, J., Díaz, J., David, D., and Landazábal, E. (2009). *Características Geomorfológicas Del Relieve Submarino En El Caribe Colombiano. En: Dimar-CIOH (Eds). Geografía Submarina Del Caribe Colombiano. Serie de Publicaciones Especiales*, Vol. 4. Colombia: CIOH, 150.
- Terry, J. P., and Goff, J. (2013). One hundred and thirty years since darwin: ‘Reshaping’ the theory of atoll formation. *Holocene* 23, 615–619. doi: 10.1177/0959683612463101
- Ui, T. (1983). Volcanic dry avalanche deposits—identification and comparison with nonvolcanic debris stream deposits. *J. Volcanol. Geotherm. Res.* 18, 135–150. doi: 10.1016/0377-0273(83)90006-9
- Vetter, E. W., Smith, C. R., and De Leo, F. C. (2010). Hawaiian hotspots: enhanced megafaunal abundance and diversity in submarine canyons on the oceanic islands of Hawaii. *Mar. Ecol.* 31, 183–199. doi: 10.1111/j.1439-0485.2009.00351.x
- Wadge, G., and Wooden, J. (1982). Late Cenozoic alkaline volcanism in the northwestern caribbean: tectonic setting and Sr isotopic characteristics: earth and planet. *Sci. Lett.* 57, 35–46. doi: 10.1016/0012-821X(82)90171-6
- Wood, J. (1996). *The Geomorphological Characterization of Digital Elevation Models*. Ph.D. thesis, University of Leicester, UK, 185.
- Yoklavich, M. M., Greene, H. G., Cailliet, G. M., Sullivan, D. E., Lea, R. N., and Love, M. S. (2000). Habitat associations of deep-water rock fishes in a submarine canyon: an example of a natural refuge. *Fish. Bull. Natl. Ocean. Atmosphere. Adm.* 98, 625–641.

**Conflict of Interest Statement:** The authors declare that the research was conducted in the absence of any commercial or financial relationships that could be construed as a potential conflict of interest.

Copyright © 2019 Idárraga-García and León. This is an open-access article distributed under the terms of the Creative Commons Attribution License (CC BY). The use, distribution or reproduction in other forums is permitted, provided the original author(s) and the copyright owner(s) are credited and that the original publication in this journal is cited, in accordance with accepted academic practice. No use, distribution or reproduction is permitted which does not comply with these terms.